

Acoustic band gaps in periodically and quasiperiodically modulated waveguides

P. D. C. King^{a)} and T. J. Cox

Acoustics Research Centre, Salford University, Salford M5 4WT, United Kingdom

(Received 9 March 2007; accepted 11 May 2007; published online 2 July 2007)

We report experimental observation of the formation of phononic band structure in one-dimensional periodically and quasiperiodically (based on the Fibonacci and Thue-Morse number sequences) area modulated waveguide structures. The experimental results are compared to model calculations considering the interference of multiply reflected waves using a transfer matrix method formulation. It was found that both the scattering due to the changes in area (causing an impedance discontinuity) and also the radiation impedance acting at each area discontinuity must be considered to accurately model the experimental results. For the quasiperiodic structures, complicated transmission spectra are seen to result, characterized by wide acoustic pseudo-band-gaps interrupted by narrow defect modes around the center of the gap. © 2007 American Institute of Physics.

[DOI: [10.1063/1.2749483](https://doi.org/10.1063/1.2749483)]

I. INTRODUCTION

Structures which have a regular distribution of scattering centers have been seen to possess a distinct and interesting array of acoustical properties, perhaps most strikingly frequency bandwidths within which sound cannot propagate through the structure—a so-called acoustic (or phononic) band gap (ABG). Such phononic crystals have been the subject of intense investigation in recent years,^{1–10} both in their own right as acoustical systems but also as an acoustical analog to the electronic behavior of crystal solids^{11,12} and the optical behavior of photonic crystals.¹³ As such, this topic forms an interesting bridge between the often uncorrelated disciplines of solid state physics, optics, and acoustics.

The scattering centers in a one-dimensional phononic crystal can be provided by a discontinuity in the open area of a rigid waveguide, and structures where these discontinuities are arranged periodically have long been known¹⁴ to provide effective filtering mechanisms for use, for example, in mechanoacoustic systems such as forced air heating, exhaust systems, and mufflers. An understanding of these systems can, however, be significantly enhanced by analyzing them as phononic crystals, rather than as lumped-element systems. A rectangular waveguide offers (under certain assumptions) a suitable system in which we can model the propagation of plane waves through a one-dimensional lossless medium. As such, they are systems which allow analytically tractable theoretical models to be verified experimentally. In this paper the acoustic transmission properties of such waveguides whose area is modulated in a periodic manner are considered; the acoustic transmission coefficient of such systems is investigated experimentally and compared to model calculations derived using a transfer matrix method (TMM).

In addition to periodic systems, structures where the scattering centers are distributed in a quasiperiodic manner are also considered. Anderson¹⁵ first showed that electronic

localization (spatial confinement of electrons in a crystal) in random media was a wave phenomena. This led to considerable interest in the localization of electromagnetic and acoustic waves in random,^{16–18} but also quasiperiodic media. The acoustical (and equivalently optical) case can be used for investigation of the fundamental properties of localization, having distinct advantages over the electronic investigation, where electron-electron and spin-orbit interactions must be incorporated. A quasiperiodic system based on the Fibonacci number sequence was investigated by x-ray diffraction and Raman scattering by Merlin *et al.*¹⁹ These structure types have since received considerable interest in the optical domain;^{20,21} the acoustical work, however, lags somewhat behind the optical work in this area. Some work has been performed on the transmission of acoustic phonons in Fibonacci superlattices^{22,23} where discrete dips in transmission have been seen. Additionally, pseudo-band-gaps have been shown (theoretically) to occur in a tube-loop structure (that is similar to a modulated waveguide) by Aynaou *et al.*²⁴ and the existence of defect modes within the pseudogap is also predicted. An experimental investigation of this phenomena is therefore warranted. This paper reports an experimental verification of these results in the audible frequency range.

II. THEORY

There are many methods with which we can model the acoustic response of a one-dimensional waveguide.^{7,9,16,22,24,25} We choose a transfer matrix method due to its flexibility. Consider a periodic system (of period Λ) of the type shown schematically in Fig. 1. The pressure, Ψ , and volume velocity U at the right of each “unit cell” can be related by a transfer matrix \mathbf{P} ²⁶

$$\begin{pmatrix} \Psi_n \\ U_n \end{pmatrix} = \mathbf{P}_n \begin{pmatrix} \Psi_{n+1} \\ U_{n+1} \end{pmatrix}, \quad (1)$$

where

^{a)}Current address: Department of Physics, University of Warwick, Coventry CV4 7AL, United Kingdom; electronic mail: philip.d.c.king@physics.org

$$\mathbf{P}_n = \begin{pmatrix} \cos(2ka_n)\cos(k\ell_n) - (S_1/S_2)\sin(2ka_n)\sin(k\ell_n) & j\rho_0c[(1/S_1)\cos(2ka_n)\sin(k\ell_n) + (1/S_2)\sin(2ka_n)\cos(k\ell_n)] \\ (j/\rho_0c)[S_2 \sin(2ka_n)\cos(k\ell_n) + S_1 \cos(2ka_n)\sin(k\ell_n)] & \cos(2ka_n)\cos(k\ell_n) - (S_2/S_1)\sin(2ka_n)\sin(k\ell_n) \end{pmatrix} \quad (2)$$

where k is the wave number, $2a_n$ is the length of the n th perturbation, S_1 (S_2) is the area of the unperturbed (perturbed) section of waveguide, and

$$\ell_n = (\Lambda_n - 2a_n) \quad (3)$$

is the length of the n th “normal” waveguide section between each perturbation where the subscript n allows for potential structure variation between each unit cell. Additionally, a radiation impedance due to the change in area can be included into the model by concatenating a transfer matrix

$$\mathbf{P}_{\text{rad}} = \begin{pmatrix} 1 & Z_{A_{\text{rad}}} \\ 0 & 1 \end{pmatrix}, \quad (4)$$

[where $Z_{A_{\text{rad}}}$ is the radiation impedance (in acoustic units) due to the fluid medium into which the acoustic wave is radiating] before and after the transfer matrix describing each perturbation of the waveguide.

Thus, the pressure and volume velocity at the left of the structure can be related to those at the right of the structure by the simple concatenation of the transfer matrices,

$$\begin{pmatrix} \Psi_0 \\ U_0 \end{pmatrix} = \left(\prod_{i=0}^{N-1} \mathbf{P}_i \right) \begin{pmatrix} \Psi_N \\ U_N \end{pmatrix}. \quad (5)$$

If all the transfer matrices are equal (the structure is locally periodic),

$$\begin{pmatrix} \Psi_0 \\ U_0 \end{pmatrix} = \mathbf{P}^N \begin{pmatrix} \Psi_N \\ U_N \end{pmatrix}, \quad (6)$$

where the transfer matrix is simply raised to the power of the number of periods in the structure. By noting that the transfer matrix \mathbf{P} is unimodular, the Cayley-Hamilton theorem can be used to determine a closed form expression for the N th power of the matrix in terms of Chebychev polynomials²⁵ and the resulting transfer matrix of the complete system,

$$\mathbf{P}^N = \begin{pmatrix} P_{11}U_{N-1}(\xi) - U_{N-2}(\xi) & P_{12}U_{N-1}(\xi) \\ P_{21}U_{N-1}(\xi) & P_{22}U_{N-1}(\xi) - U_{N-2}(\xi) \end{pmatrix}, \quad (7)$$

where P_{ij} are the (i, j) elements of the single period transfer matrix, $U_N(\xi)$ is the Chebychev polynomial of the second kind,

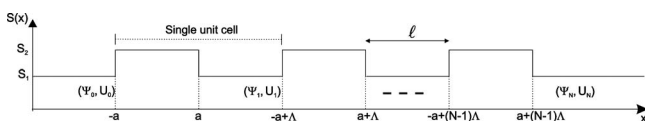


FIG. 1. Schematic representation of N periodic repetitions (of period length Λ) of abrupt expansions (of length $2a$) and contractions in a waveguide.

$$U_N(\xi) = \frac{\sin[(N+1)\gamma]}{\sin \gamma}, \quad (8)$$

where

$$\gamma = \cos^{-1}(\xi), \quad (9)$$

and ξ is related to the trace of the single period transfer matrix

$$\xi = \frac{1}{2} \text{Tr}(\mathbf{P}). \quad (10)$$

From the total transfer matrix, the intensity transmission and reflection coefficients can be easily calculated.

III. EXPERIMENTAL DETAILS

The basic waveguide structure used in this work is formed from an impedance tube (rigid rectangular plane walled metal tube). The total waveguide length (from loudspeaker to measurement position) is 3 m, and the waveguide is terminated with an anechoic termination behind the measurement position to prevent reflections from the end of the tube. Reflections from the source (loudspeaker) end of the waveguide, reflecting waves that were previously reflected from the modulated structure, were also problematic. These were partially removed by inserting some loosely packed fibrous absorbent at this end of the tube.

The internal dimensions of each waveguide section are square with side length of 54.0 ± 0.5 mm. This places an upper limit on the range of validity of the measurements as the analysis assumes that plane waves propagate within the tube. For a square tube, this gives an upper limiting frequency²⁷ of approximately 3 kHz.

The cross-sectional area of the waveguide is modulated by inserting rigid aluminium blocks into the waveguide. The blocks have square cross section with side length 38 mm, giving a ratio of areas in the waveguide of $\eta = S_1/S_2 = 2.02$. The resulting waveguide is no longer square when the perturbations are present. This is not, however, important at the frequency ranges considered as the plane wave limit applies. Vaseline is used on the surfaces of the block in contact with the waveguide structure to ensure a good seal and to avoid any absorption effects that would be associated with small gaps between the blocks and the original waveguide structure. It was found that identical results were obtained if the blocks were placed in contact with two edges or if placed in contact with only one edge of the original waveguide structure.

The measurements were performed using a maximum length sequence (MLS) signal to generate an impulse and frequency response of the structure.²⁸ The system was excited with a standard loudspeaker. The MLS signal, after propagating through the structure, was received by a 1/4 in.

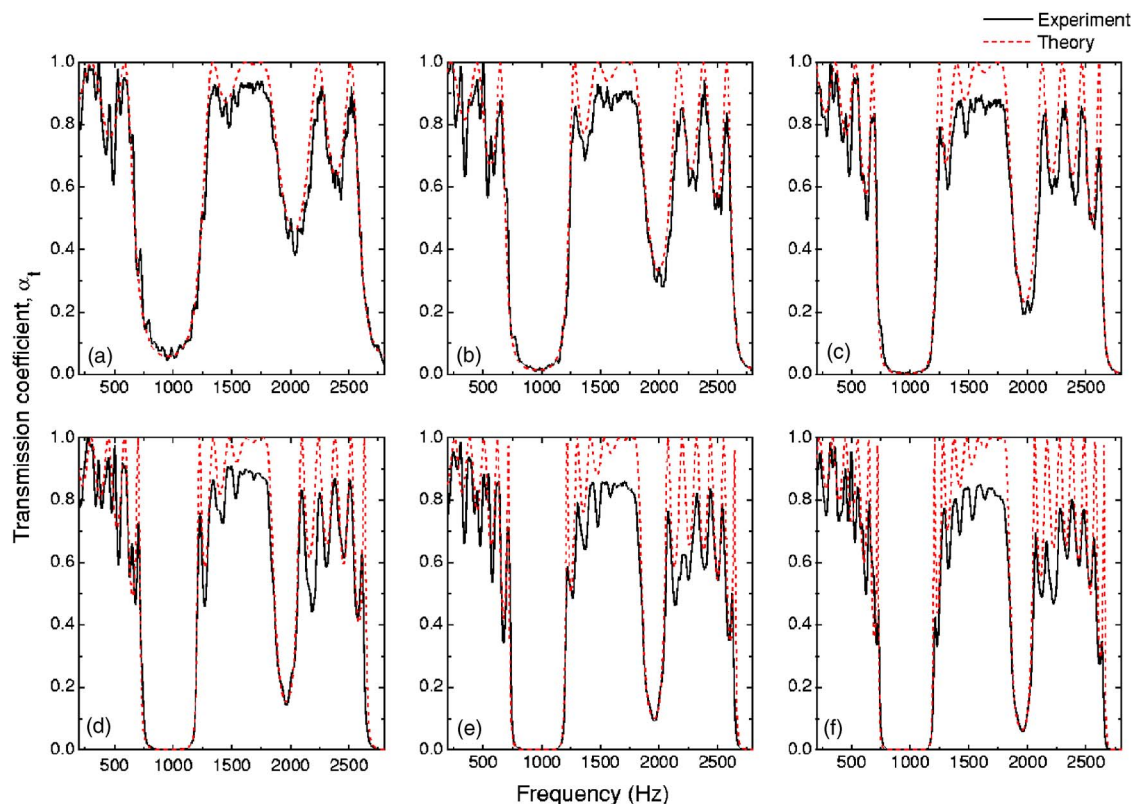


FIG. 2. (Color online) The measured intensity transmission coefficient of a three to eight [(a)–(f)] period Bragg stack (solid line) with period $\Lambda=0.172$ m. The theoretical modeling results (dashed line) are also shown including a radiation impedance $Z_{A_{\text{rad}}}=4j\omega$ at each area discontinuity. A good agreement is seen between the measured and theoretical results with clear acoustic band gaps forming for the higher numbers of periods.

free field microphone, which has a flat frequency response (to within 1 dB) between 10 Hz and 40 kHz. This was connected to a preamplifier and then a measuring amplifier before being captured by the computer's sound card.

IV. PERIODIC SYSTEMS

A. Results and modeling

Initially, the waveguide structure was constructed in a periodic arrangement of the form shown in Fig. 1 with a period length of $\Lambda=0.172$ m and a perturbation length $2a=\Lambda/2$. This arrangement will be termed a Bragg stack in analogy with the familiar optical Bragg stacks.²⁹ The measured intensity transmission coefficient for varying numbers of periods of the Bragg stack is shown in Fig. 2.

For all numbers of periods, the transmission shows a complex nonmonotonic dependence on the frequency, with significant dips around 1 kHz and slightly less well defined dips around 2 kHz. A further significant dip is seen at higher frequencies (approximately around 3 kHz), although this dip cannot be fully resolved due to the plane wave limit of the waveguide. The large dips in frequency are seen to become deeper and flatter with increasing numbers of periods and, above approximately six periods, form complete band gaps in the material—extended regions of frequency in which acoustic waves cannot propagate through the structure. Between each of the large dips in transmission, significant interference fringes are observed.

The theoretical modeling of transmission through the Bragg stacks are also shown in Fig. 2. In order to achieve

agreement between the experimental and theoretical results, it was found necessary to include the radiation impedance which naturally occurs at every change in cross-sectional area. Without the radiation impedance, the dip at ~ 2 kHz is not predicted.

In a lumped-element approximation, at the change in area, the air acts as a plane piston, and the radiation impedance acts on this piston. The radiation impedance is modified by the periodicity both perpendicular (due to image sources) and parallel to the sidewalls of the waveguide structure; standard formulations²⁶ are therefore not applicable. Consequently, the value of the radiation impedance was estimated from the experimental results, and good agreement was found with a value of $Z_{A_{\text{rad}}}=4j\omega$.

Including this *mass loading* effect (radiation impedance), good agreement is seen between the experimental data and the theoretical predictions for all numbers of periods of the structure. It should be noted that, for small numbers of periods, the transmission coefficients display some small oscillatory behavior not theoretically present and not observed with larger numbers of periods. It was found experimentally that this was due to reflections from the loudspeaker at the source end of the waveguide. The extra oscillations seen in the transmission coefficients of modulated waveguides with a low number of periods (with respect to the theoretical predictions) can therefore be judged to be due to experimental error, and not theoretical inaccuracies. In addition, the magnitude of the measured transmission coefficient peaks is slightly lower than that of the theoretical results. This is due

to losses in the medium, which was treated as lossless in the modeling.

B. Discussion

Significant insight can be gained into these results by considering the waveguide structure in the infinitely periodic limit. Invoking the Bloch-Floquet theorem,^{30,31} the wavefunction (pressure) at a location x is given by

$$\psi_K(x) = e^{\pm iKx} u_K(x), \quad (11)$$

where K is the Bloch wave vector and $u_K(x)$ is the Bloch function which is a function with the periodicity of the structure,

$$u_K(x + \Lambda) = u_K(x). \quad (12)$$

Using this condition, and Eq. (1), it can be shown that the Bloch wave vector is given by

$$K = \frac{1}{\Lambda} \cos^{-1} \xi, \quad (13)$$

where ξ is defined by Eq. (10).

If $|\xi| < 1$, K is entirely real and so the Bloch waves are propagating waves. Thus, acoustic waves incident on the phononic crystal with frequencies such that $|\xi| < 1$ are able to propagate through the structure, and this therefore corresponds to allowed energy bands in the structure. If, however, $|\xi| > 1$, K is complex and the Bloch waves are evanescent (they decay exponentially with distance into the phononic crystal). Therefore, frequencies such that $|\xi| > 1$ correspond to forbidden energy bands within the phononic crystal (i.e., to band gaps, regions where propagation is not allowed). Indeed, by further mapping the real component of the Bloch wave number in terms of frequency, a plot of the band structure can be built up, showing the dispersion relation of the medium and the allowed and forbidden bands. Although this analysis only holds for an infinitely periodic medium, it provides insight into the transmission properties of the locally periodic structures investigated here.

The band structure for the Bragg stack considered here is shown in the reduced zone scheme in Fig. 3. Regions of frequency (for example, around 1 kHz) can be clearly seen where there is no allowed solution of the Bloch wave vector (a gap is seen between the allowed states). This corresponds to the band gaps of the structure, and comparison with Fig. 2 shows that these gaps occur over the same frequency range as the transmission stop bands are forming. In these regions, the Bloch wave number is complex, leading to an evanescent wave and hence zero transmission (for the infinite structure). Thus, the dispersion relation of the structure can be seen to be separated into allowed bands separated by forbidden regions, or band gaps. As the number of periods is increased, the decay of the evanescent waves through the structure is more complete, leading to the acoustic band gaps forming more fully.

A simple qualitative justification of these band gaps can also be given. At each discontinuity in the area of the structure, the incident wave is partially reflected. If the reflected waves are in phase with each other, a standing wave will be

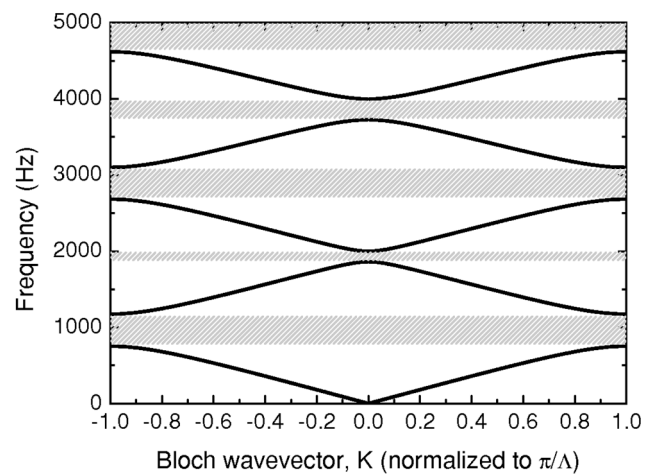


FIG. 3. The band structure for the infinitely periodic Bragg stack system with period $\Lambda=0.172$ m and a radiation impedance $Z_{A,\text{rad}}=4j\omega$ acting every $\Lambda/2$. Acoustic band gaps (where no acoustic waves can propagate) are represented by shading.

formed, and sound will not propagate through the material leading to the formation of band gaps.^{9,32} The frequencies at which the reflected waves are exactly in phase are the center frequencies of the band gaps, $f_c=c/2\Lambda, 3c/2\Lambda, \dots$, justifying the formation of the band gaps observed here at ~ 1 and ~ 3 kHz. Conversely, when the period length is not close to a half-wavelength of the incident wave, the reflected waves are not in phase, a standing wave is not formed, and so sound at these frequencies can propagate through the structure (with some attenuation depending on the exact interference of incident and reflected waves).

The band gap at ~ 2 kHz can be understood by considering the radiation impedance. This occurs at every change of cross-sectional area, i.e., with a periodicity that is half that of the main structure. This therefore introduces small (due to the small magnitude of the impedance) band gaps to open up at ~ 2 kHz (i.e., twice the center frequency of the primary band gap reflecting the reduced period length). Note, with the current period length, the fundamental band gap would be expected, from the above discussion, to open up centered at exactly 1 kHz. However, there is an effective increase in length of each perturbation in the waveguide by end corrections due to the radiation impedance.³³ This causes a slight decrease to the exact center frequencies of the band gaps, as observed here.

V. FIBONACCI SYSTEMS

Systems based on the Fibonacci number sequence (FS) were also investigated in this work. In the current context, such systems are composed of layers denoted as A and B of cross-sectional area S_1 and S_2 , respectively (where B therefore denotes a perturbation to the original waveguide), where the layer sequence of the structure (of order n) is given by the recursion relation

$$S_n = \{S_{n-1}, S_{n-2}\}, \quad (14)$$

with

TABLE I. The sequence of the Fibonacci multilayer structure definitions up to seventh order. A denotes a “normal” section of waveguide and B a section with a perturbed cross section (i.e., an expansion or contraction in the waveguide).

Symbol	Fibonacci layer sequence	No. of layers
S_0	B	1
S_1	A	1
S_2	BA	2
S_3	ABA	3
S_4	$BAABA$	5
S_5	$ABABAABA$	8
S_6	$BABAABABAABA$	13
S_7	$ABABAABABAABAABAABA$	21

$$S_0 = \{B\},$$

$$S_1 = \{A\}.$$

The sequence of the Fibonacci multilayer structure definitions up to seventh order is given in Table I.

A. Results and modelling

The measured transmission coefficients for single period Fibonacci structures, with a single (A or B) layer thickness of 0.086 m, of order four to seven are shown in Fig. 4.

The interference of acoustic waves scattered from the discontinuities in the waveguide now combine to give a more complicated transmission spectrum than in the case of the

periodic Bragg stack considered above. Clear pseudogaps can be seen to result. Note, these are termed pseudogaps as the medium is not periodic, and so full band gaps (as defined by the Bloch phase) do not form. The gaps occur spaced around the central frequency of the band gap that would result from a Bragg stack with the same layer thicknesses (~ 1 kHz). The pseudogaps form more fully as the order of the FS structure is increased, with full pseudogaps only forming for the highest order structure investigated here. Note, a dip in transmission is seen to form at ~ 2 kHz as for the periodic structures. This is due to the radiation impedance effects discussed previously.

Including the mass loading effects, with the same value for the radiation impedance as used for the periodic structures, good general agreement is achieved between the experimental and theoretical results. For low orders of structure sequence, the measured transmission coefficient can be seen to display extra oscillations that are not present in the theoretical results. These can again be explained by small reflections from the loudspeaker. The experimental and theoretical results show good qualitative agreement with the theoretical calculations for the FS tube-loop structure (a similar configuration to that used here) of Aynaou *et al.*²⁴

For the higher order structures, the higher values of transmission can be seen to be reduced somewhat below their theoretical values. This is most likely due to absorption within the waveguide structure, which is more important for the higher order structures as the propagation distance is much longer (the structures are much larger). The central

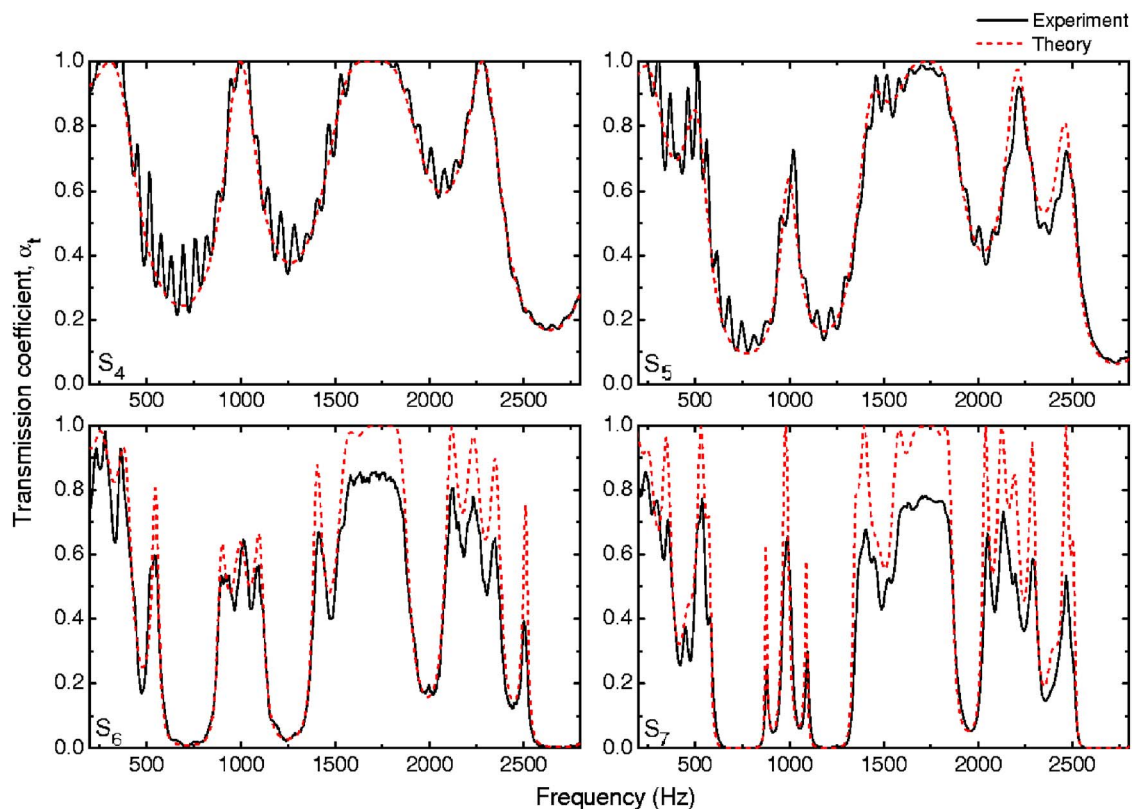


FIG. 4. (Color online) The measured intensity transmission coefficient (solid line) for fourth, fifth, sixth, and seventh order FS modulated waveguide structures. The theoretical modeling results (dashed line) are also shown including a radiation impedance $Z_{A,rad} = 4j\omega$ at each area discontinuity. Good general agreement is seen between the measured and theoretical results.

transmission peak of the seventh order FS system is substantially reduced below the theoretical value. This will be discussed in further detail below.

B. Discussion

The structures considered here are quasiperiodic—indeed, their autocorrelation functions are strongly peaked at delays equal to the Fibonacci numbers. It has been shown³⁴ that this quasiperiodicity (where some periodicity exists along with some disorder) results in sets of critical states with transmission coefficient $0 < \alpha_i < 1$ which correspond to states intermediate between extended periodic Bloch states ($\alpha_i = 1$) and fully disordered (Anderson) localized states ($\alpha_i = 0$). Thus, bands of allowed and forbidden states still form leading to the pseudo-band-gaps seen here.

Three regions warrant specific consideration. First, in the middle of allowed bands, extended Bloch-like states are formed and the transmission therefore approaches unity, as seen in Fig. 4. Second, at the band edges (~ 600 and ~ 1400 Hz for the first band gap in the current case) band edge resonances have been shown to occur in optical Fibonacci structures³⁵ which decay by a power law. Analysis of the local density of states by Aynaou *et al.*²⁴ shows that these states show a marked similarity to band edge states in a periodic structure. Thus, these states can be seen to mark a transition from periodic properties (band gaps) to disorder induced properties (critically localized states). The power law decay of these states compared to the exponential decay of the gap states results in an increase of transmission, as in finite length structures, the field does not decay to zero.

Third, the middle of the pseudogap deserves attention. States at these frequencies have been shown to exhibit a self-similar behavior around the central peak, providing evidence of critical localization of these states, rather than extended or Anderson localized states forming. Note, the theoretical calculations used in this work exhibit this self-similar behavior, although due to experimental size constraints, sufficiently larger structures could not be constructed to display this self-similarity experimentally. These critically localized states are largely equivalent to the defect states introduced when a periodic system is perturbed by a defect element.^{9,32} The number of defect peaks observed in the FS structure pseudogaps increases with increasing order of the structure. Due to their localized nature, waves propagating within these defect modes are expected²⁴ to have a slower group velocity than waves propagating through the unmodulated plane waveguide. The increasing numbers of defect modes with increasing order of the structure would therefore lead to extended frequency bands within which the speed of sound in the tube may be reduced below its standard value. This is in contrast to the anomalous dispersion that occurs within the band gaps increasing the group velocity above the speed of sound in an unmodulated waveguide.

As a simple example, the defect transmission exactly at the center of the gap can be analyzed analytically. At this frequency, a “double thickness” layer (AA or BB) is one-half wavelength thick and therefore has no effect on propagation

of acoustic waves. At this frequency, the S_6 structure, for example, can therefore be reduced as follows:

$$BAABAABABAABA \rightarrow BBBABBA \rightarrow BAA = B. \quad (15)$$

Thus, at f_c , the structure acts as if it is composed of only a single B layer, equivalent to a single period of the Bragg stack considered previously, resulting in the only partially reduced transmission seen at this frequency. The other defectlike peaks are more difficult to analyze directly, but result due to the exact interference conditions between reflections from each discontinuity in the area of the structure. This holds for the S_5 structure also. Conversely, the S_4 and S_7 structures reduce, at f_c , to a single unperturbed (A) layer, and therefore perfect transmission would be expected. This is seen to occur in the modeling results at this frequency and is seen in the S_4 experimental results.

The nature of these defect states also explains the significant differences in magnitude between the theoretical and measured transmission at f_c in the S_7 structure. The perfect transmission holds only for acoustic waves propagating through the structure at exactly f_c leading to a narrow defect peak. However, if there is some small variation in the spacings of the blocks, there is some variation in the frequencies that couple to this defect mode, thus reducing the magnitude of the transmission at f_c and reducing the Q factor and height of the defect peak with respect to the theoretical value.

VI. THUE-MORSE SYSTEMS

It has previously been seen in electronic systems that structures based on similar sequences such as the Thue-Morse sequence display quasiband structure due to extended and critically localized modes as in the Fibonacci system.³⁶ Two structures based on this sequence are therefore briefly considered here.

In the current study, the Thue-Morse (TM) structure sequence is defined by the recursion relation

$$S_n = \{S_{n-1}, S_{n-1}^+\} \quad n \geq 1, \quad (16)$$

where S_n^+ denotes a second recursion relation

$$S_n^+ = \{S_{n-1}^+, S_{n-1}\}, \quad (17)$$

with

$$S_0 = \{A\},$$

$$S_0^+ = \{B\}.$$

The sequence of the TM multilayer structure definitions up to fifth order are shown in Table II.

The measured transmission coefficients for single period TM structures, with a single (A or B) layer thickness of 0.086 m, of order three and four are shown in Fig. 5. Pseudogaps are indeed seen to form for these structures, but these are interrupted by more defect peaks than was observed in the FS structures. This is consistent with the TM layer sequence being more aperiodic than the Fibonacci layer sequence³⁷ (its Fourier spectrum is more continuous). The greater degree of disorder leads to more modes which are critically localized, leading to a wider frequency range of

TABLE II. The sequence of the TM multilayer structure definitions up to fifth order. *A* denotes a normal section of waveguide and *B* a section with a perturbed cross section (i.e., an expansion or contraction in the waveguide).

Symbol	Thue-Morse layer sequence	No. of layers
S_0	<i>A</i>	1
S_1	<i>AB</i>	2
S_2	<i>ABBA</i>	4
S_3	<i>ABBABAAB</i>	8
S_4	<i>ABBABAABBAABABBA</i>	16
S_5	<i>ABBABAABBAABBABAABABBAABBAAB</i>	32

transmission (defect) peaks within the gap than in the FS structures. The number of these defect peaks increases with increasing order of structure (as there are more possible interference paths that give rise to high transmission through the structure due to destructive interference of the back reflected waves). As with the other structures investigated, the pseudogaps become deeper and more clearly defined with increasing order of the structure, as would be expected due to its increased length.

VII. CONCLUSIONS

One-dimensional periodically and quasiperiodically modulated waveguides have been examined experimentally

and theoretically. While one-dimensional phononic crystals have been examined before, previous work has not provided a detailed comparison of experimental and theoretical results. The results were accurately modeled by considering the interference of multiply reflected waves through the structure. Acoustics is unusual in having to consider radiation impedance. It was shown to be necessary to consider scattering caused by this radiation impedance, in addition to the scattering caused by the impedance discontinuity due to the change in volume velocity at each change in area of the waveguide, to gain good agreement between measurement and theory. Also, the introduction of another source of periodicity potentially offers the opportunity to develop additional band gaps. For Fibonacci structures, a complicated transmission spectrum was seen to result, characterized by wide acoustic pseudoband gaps interrupted by narrow defect modes at the center of the gap. This was discussed in terms of the existence of critically localized modes within the structure. Similar transmission spectra were observed for structures based on the Thue-Morse number sequence. This work therefore provides experimental verification of the transmission properties of one-dimensional phononic crystals based on the quasiperiodic Fibonacci and Thue-Morse number sequences.

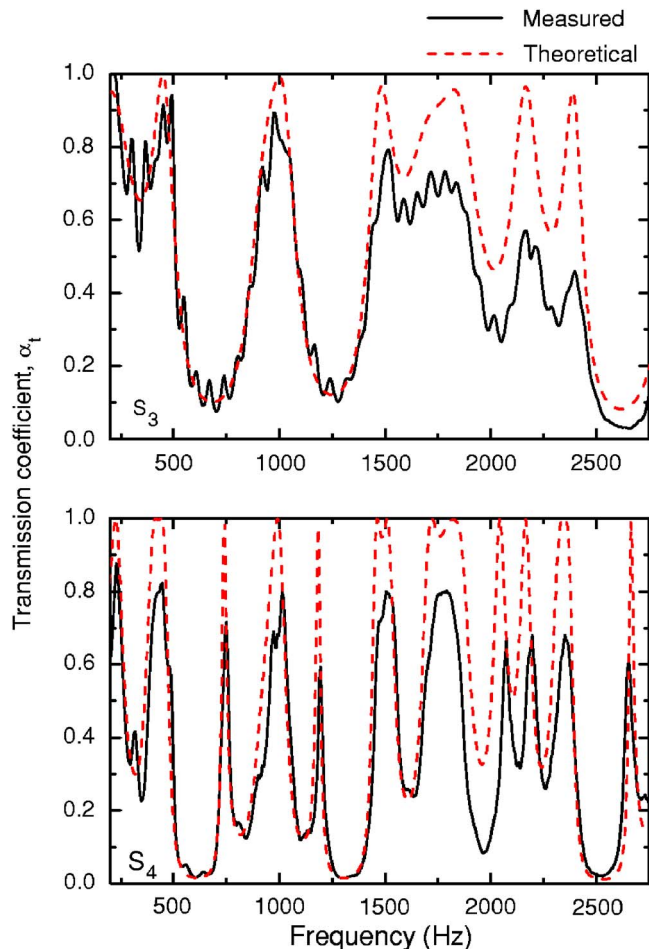


FIG. 5. (Color online) The measured intensity transmission coefficient (solid line) for third and fourth order TM modulated waveguide structures. The theoretical modeling results (dashed line) are also shown including a radiation impedance $Z_{rad} = 4j\omega$ at each area discontinuity. Good general agreement is seen between the measured and theoretical results.

- ¹J. P. Dowling, *J. Acoust. Soc. Am.* **91**, 2539 (1992).
- ²M. Sigalas and E. N. Economou, *Solid State Commun.* **86**, 141 (1993).
- ³R. Martínez-Sala, J. Sancho, J. V. Sánchez, G. V. J. Llinares, and F. Meseguer, *Nature (London)* **378**, 241 (1995).
- ⁴M. S. Kushwaha and P. Halevi, *J. Acoust. Soc. Am.* **101**, 619 (1997).
- ⁵M. S. Kushwaha, *Appl. Phys. Lett.* **70**, 3218 (1997).
- ⁶W. M. Robertson and J. F. Rudy III, *J. Acoust. Soc. Am.* **104**, 694 (1998).
- ⁷C. E. Bradley, *J. Acoust. Soc. Am.* **96**, 1844 (1994).
- ⁸C. E. Bradley, *J. Acoust. Soc. Am.* **96**, 1854 (1994).
- ⁹J. N. Munday, C. B. Bennett, and W. M. Robertson, *J. Acoust. Soc. Am.* **112**, 1353 (2002).
- ¹⁰S. Chen, T. Tang, and Z. Wang, *Acta. Acust. Acust.* **93**, 31 (2007).
- ¹¹R. de L. Kronig and W. G. Penney, *Proc. R. Soc. London, Ser. A* **130**, 499 (1931).
- ¹²N. W. Ashcroft and N. D. Mermin, *Solid State Physics* (Harcourt College, London, 1976).
- ¹³E. Yablonovitch, *Phys. Rev. Lett.* **58**, 2059 (1987).
- ¹⁴L. E. Kinsler, A. R. Frey, A. B. Coopens, and J. V. Sanders, *Fundamentals of Acoustics*, 3rd ed. (Wiley, New York, 1982).
- ¹⁵P. W. Anderson, *Phys. Rev.* **109**, 1492 (1958).
- ¹⁶V. Baluni and J. Willemsen, *Phys. Rev. A* **31**, 3358 (1985).
- ¹⁷D. Sornette and O. Legrand, *J. Acoust. Soc. Am.* **92**, 296 (1992).
- ¹⁸P. Luan and Z. Ye, *Phys. Rev. E* **63**, 066611 (2001).
- ¹⁹R. Merlin, K. Bajema, R. Clarke, F. Y. Juang, and P. K. Bhattacharya, *Phys. Rev. Lett.* **55**, 1768 (1985).
- ²⁰M. Kohmoto, B. Sutherland, and K. Iguchi, *Phys. Rev. Lett.* **58**, 2436 (1987).
- ²¹W. Gellermann, M. Kohmoto, B. Sutherland, and P. C. Taylor, *Phys. Rev. Lett.* **72**, 633 (1994).
- ²²S. Tamura and J. P. Wolfe, *Phys. Rev. B* **36**, 3491 (1987).
- ²³S. Tamura and J. P. Wolfe, *Phys. Rev. B* **38**, 5610 (1988).
- ²⁴H. Aynaou, E. H. El Boudouti, B. Djafari-Rouhani, A. Akjouj, and V. R. Velasco, *J. Phys.: Condens. Matter* **17**, 4245 (2005).
- ²⁵D. J. Griffiths and C. A. Steinke, *Am. J. Phys.* **69**, 137 (2001).
- ²⁶T. J. Cox and P. D'Antonio, *Acoustic Absorbers and Diffusers: Theory, Design and Application* (Spon, London, 2004).
- ²⁷British Standards Institution, BS EN ISO 10534-1:2001, Acoustics—Determination of sound absorption coefficient and impedance in impedance tubes. Part 1: Method using standing wave ratio, BSI (2001).
- ²⁸WINMLS, Morset Sound Development, 2004, <http://www.winmls.com>.
- ²⁹G. Brooker, *Modern Classical Optics*, Oxford Master Series in Atomic, Optical and Laser Physics (Oxford University Press, Oxford, 2003).
- ³⁰F. Bloch, *Z. Phys.* **52**, 555 (1928).

- ³¹G. Floquet, *Ann. Sci. Ec. Normale Super.* **12**, 47 (1883).
- ³²P. D. King, M.S. thesis, University of Salford, 2006.
- ³³L. L. Beranek, *Acoustics* (Acoustical Society of America, New York, 1996).
- ³⁴E. Maciá and F. Domínguez-Adame, *Phys. Rev. Lett.* **76**, 2957 (1996).
- ³⁵L. D. Negro *et al.*, *Phys. Rev. Lett.* **90**, 055011 (2003).
- ³⁶A. Chakrabarti, S. N. Karmakar, and R. K. Moitra, *Phys. Rev. Lett.* **74**, 1403 (1995).
- ³⁷P. W. Mauriz, E. L. Albuquerque, and M. S. Vasconcelos, *Phys. Rev. B* **63**, 184203 (2001).